

# A Study of the Optical Properties in ZnWO<sub>4</sub> Nanorods Synthesized by Hydrothermal Method<sup>#</sup>

Nguyen Van Minh<sup>1\*</sup>, Nguyen Manh Hung<sup>1,2</sup>

<sup>1</sup>Center for Nano Science and Technology, and Department of Physics, Hanoi National University of Education, Hanoi, Vietnam; <sup>1,2</sup>Hanoi University of Mining and Geology, Dong Ngac, Tu Liem, Hanoi, Vietnam.  
Email: \*minhvn@hnue.edu.vn; minhsp@gmail.com

Received May 17<sup>th</sup>, 2011; revised April 20<sup>th</sup>, 2011; accepted June 7<sup>th</sup>, 2011.

## ABSTRACT

We investigate the effect of synthesized time on the structure, as well as optical properties in ZnWO<sub>4</sub> nano rod prepared by hydrothermal method. The prepared rods were characterized by X-ray diffraction (XRD), scanning electron microscopy (SEM), Raman scattering, absorption and photoluminescent (PL) spectra techniques. The size and morphology of ZnWO<sub>4</sub> nano-rod can be controlled by adjusting the reaction time. The resultant sample is a pure phase of ZnWO<sub>4</sub> without any impurities. The results showed that the optical property of ZnWO<sub>4</sub> nanoparticles obviously relied on their rod sizes.

**Keywords:** ZnWO<sub>4</sub> Nano Rod, Raman Spectroscopy, Absorption, Photoluminescence

## 1. Introduction

Zinc tungstate (ZnWO<sub>4</sub>) with a wolframite structure has been of practical interest for a long time because of its attractive luminescence [1]. ZnWO<sub>4</sub> has been applied as a possible new material for microwave amplification by stimulated emission of radiation [2], scintillator [3] and optical hole burning lattice material [4], etc. Recently, new applications for this material have emerged, including large-volume scintillators for high-energy physics [5]. In particular, ZnWO<sub>4</sub>, also known by its mineral name sanmartinite, is a wide-gap semiconductor, with band gap energy close to 4 eV [6], and is a promising material for the new generation of radiation detectors.

ZnWO<sub>4</sub> has been prepared by different routes such as the Czochralski method [7], sintering of WO<sub>3</sub> and ZnO or ZnCO<sub>3</sub> powders [8], reaction in aqueous solution followed by heating of the precipitate [9], heating of ZnO thin films with WO<sub>3</sub> vapor [10], sol-gel reaction [11], and hydrothermal reaction over an extensive period [12]. However, ZnWO<sub>4</sub> particles prepared by these routes are relatively large in particle size and irregular in morphology. Furthermore, higher calcining temperature is still needed. It is very significant whether in fundamental or applied field to explore new routes to ZnWO<sub>4</sub>, especially for ZnWO<sub>4</sub> crystallites with nanometer size, which would

have unique properties compared to traditional products [13,14]. To obtain nanosized powders, the solid state methods have several problems, because the WO<sub>3</sub> has a tendency to vaporize at high temperatures [15], nonhomogeneous compounds might be easily formed during the solid-state and melting processing and the temperature for the solid state reaction is relatively high [16]. These problems could be solved by applying the hydrothermal method. However, a few studies on the chemical synthesis of zinc tungstate by the hydrothermal method have been reported. Furthermore, very few papers were concerned with effects of the size and morphology on the optical properties of ZnWO<sub>4</sub> nanoparticles.

In this work, we report the synthesis of ZnWO<sub>4</sub> nano rod by hydrothermal method at a low temperature of 180°C and investigate their structure, Raman scattering, absorption and photoluminescence.

## 2. Experiment

Zinc tungstate (ZnWO<sub>4</sub>) nanoparticles were prepared by the hydrothermal reaction of Zn(NO<sub>3</sub>)<sub>2</sub>·6H<sub>2</sub>O and Na<sub>2</sub>WO<sub>4</sub>·2H<sub>2</sub>O at temperature of 180°C, and various reaction times (2, 4, 6 and 8 h). In a typical procedure for the preparation of sample, Zn(NO<sub>3</sub>)<sub>2</sub>·6H<sub>2</sub>O (1 mmol) in water (10 ml) was added Na<sub>2</sub>WO<sub>4</sub>·2H<sub>2</sub>O (1 mmol) in water (20 ml) with vigorous stirring. H<sub>2</sub>O was added to make 40 ml of the solution, and pH of the solution was

<sup>#</sup>This work has been supported by The Vietnam's National Foundation for Science and Technology Development (NAFOSTED).

adjusted to 6.68, respectively, with dilute of 30% NH<sub>3</sub>·H<sub>2</sub>O solution. The solution was then added into a Teflon-lined stainless steel autoclave of 100 ml capacity. The autoclave was heated to 180°C for 2, 4, 6 and 8 h, respectively, without shaking or stirring. Afterwards, the autoclave was allowed to cool to room temperature gradually. The white precipitate collected was washed with distilled water four times. The solid was then heated at 80°C and dried under vacuum for 2.5 h.

Structural characterization was performed by means of X-ray diffraction using a D5005 diffractometer with Cu K $\alpha$  radiation. The FE-SEM observation was carried out by using a S4800 (Hitachi) microscope. Raman measurements were performed in a back scattering geometry using Jobin Yvon T 64000 triple spectrometer equipped with a cryogenic charge-coupled device (CCD) array detector, and the 514.5 nm line of Ar ion laser. The absorption spectra were recorded by using Jasco 670 UV-vis spectrometer and the room temperature luminescent spectra were recorded on a spectrofluorometer (PL, Fluorolog-3, Jobin Yvon Inc, USA).

### 3. Result and Discussion

#### 3.1. Structure

**Figure 1** shows the XRD patterns of ZnWO<sub>4</sub> powders heated for 2, 4, 6 and 8 h as a function of the reaction time. It is noted that the ZnWO<sub>4</sub> single phase could be observed in all XRD patterns. All diffraction peaks of ZnWO<sub>4</sub> crystal appeared when the sample was prepared at 180°C, which could be easily indexed as a pure, monoclinic wolframite tungstate structure according to the standard card (JCPDS Card number: 73-0554). It was found that, the optimum temperature for the production

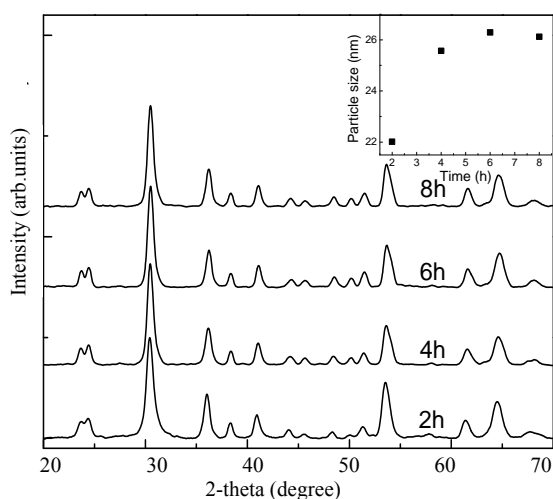


**Figure 1.** XRD patterns of nanosamples with various reaction times. The inset shows the particle size vs. reaction time.

of the high-quality crystal was as high as 180°C [17].

The morphologies and microstructures of the samples were then investigated with SEM. **Figure 2** shows that the morphologies and dimensions of the samples were strongly dependent on the reaction time. SEM micrograph for the sample synthesized for 2 h was basically irregular (**Figure 2a**). With the increase of the reaction time to 4 h, the rod-shaped crystals can be seen (**Figure 2b**), and the rod size was in the range from several nanometers to several tens of nanometers. For 6 h, the crystal was basically rod-like (**Figure 2c**). When the reaction time was raised to 8 h, the rod-shaped crystals grew larger and longer and a majority of the crystals have exceeded 50 nm in length, the sizes of the rods became homogeneous (**Figure 2d**). However, it was shown that, for longer reactive times, such as 48 h, the crystal phase instead became inhomogeneous, which could be due to the breakage of the large crystal under such conditions, suggesting the worse crystallinity [12]. The inset of **Figure 1** shows the average crystallite sizes for the heat-treated powders calculated by XRD line broadening method [18]. The calculated average crystallite sizes were 22.02, 25.00, 26.05 and 26.00 nm for the heat-treated powders at 2, 4, 6 and 8 h, respectively. These are corresponding to the SEM observation in **Figure 2** showing an ordinary tendency to increase with the reaction time from 2 h to 8 h. However, Zhao *et al.* [19] has investigated the calcinations time and concluded that the calcination time plays little effect on the crystal phase of ZnWO<sub>4</sub>. This comment was contrary to our result.

#### 3.2. Absorption Spectroscopy

**Figure 3** shows a diffuse reflection spectrum of ZnWO<sub>4</sub> nanopowder. Steep shape of the spectra indicated that the UV light absorption was due to the band-gap transition instead of the transition from the impurity level. For a

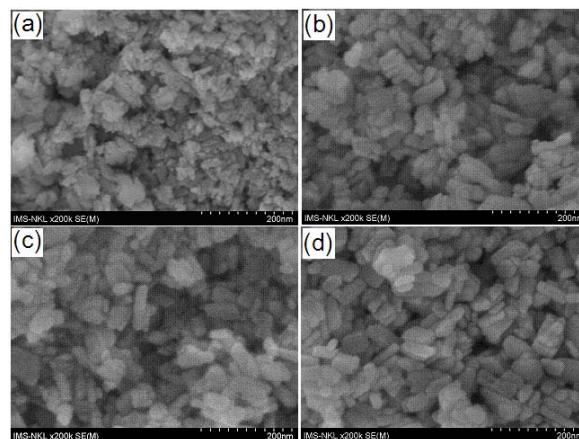


**Figure 2.** SEM images of the nanosamples synthesized in different time: for 2 h (a), 4 h (b), 6 h.

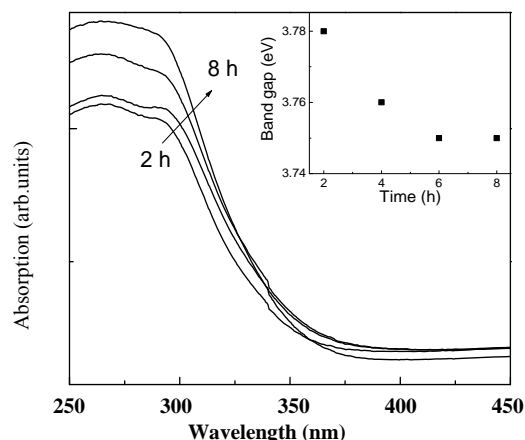


**Figure 3.** Diffuse reflection spectra of ZnWO<sub>4</sub> nanopowders. The inset shows the optical band gap vs. reaction time.

crystalline semiconductor, the optical absorption near the band edge follows the equation:  $ah\nu = A(h\nu - E_g)^{1/n}$ , where  $a$ ,  $\nu$ ,  $E_g$  and  $A$  are absorption coefficient, light frequency, band gap, and a constant, respectively [20]. For the ZnWO<sub>4</sub>,  $n$  is determined to be 2. Thus, the band gaps of the ZnWO<sub>4</sub> nanopowders were roughly estimated to be 3.78, 3.76, 3.73 and 3.72 eV, as shown in the inset of **Figure 3**. Bonanni *et al.* [21] reported that the band gap of ZnWO<sub>4</sub> was 3.75 eV, which is in agreement to our experimental values. However, the band gap becomes narrower in the sample with longer reaction time. Therefore, the crystallization degree may contribute to the absorption edge shift.

### 3.3. Raman Spectroscopy

**Figure 4** illustrates the Raman spectra for ZnWO<sub>4</sub> nanopowders. It is clear that, the peak shifts to higher frequency as increasing the reaction time. Studies of the optical properties and the Raman spectra of ZnWO<sub>4</sub> at room temperature have been reported in the literature [22]. ZnWO<sub>4</sub> has the monoclinic wolframite structure

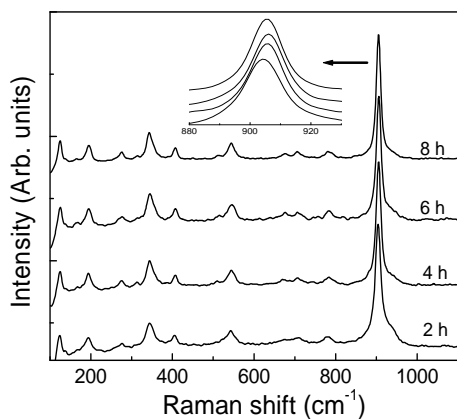


**Figure 4.** Raman spectra of ZnWO<sub>4</sub> nanopowders.

with C<sub>2h</sub> point group symmetry and P2/c space group. It has two formula units per unit cell. The W-O interatomic distance is substantially smaller than that of Zn-O, therefore, to a first order approximation, the lattices can be separated into internal vibrations of the octahedra and the external vibrations in which an octahedron vibrates as a unit. A group theoretical calculation of the ZnWO<sub>4</sub> structure yields 36 lattices modes, of which 18 are Raman active (8A<sub>g</sub> + 10B<sub>g</sub>).

It is assigned to the A<sub>g</sub> mode observed near 907 cm<sup>-1</sup> since, as is the case of the regular octahedron, the symmetric stretch is expected to have the highest frequency of all the internal modes. The E<sub>g</sub> mode (asymmetric stretch) of the regular octahedron splits into A<sub>g</sub> + B<sub>g</sub> by the crystal field. Again, these modes are expected to have frequencies that are higher than those of the bending mode (T<sub>2g</sub>) of the regular octahedron. The obvious choices are the B<sub>g</sub> and A<sub>g</sub> modes observed near 786 and 709 cm<sup>-1</sup>, respectively. The remaining modes 2A<sub>g</sub> + B<sub>g</sub> with frequencies of 407, 342 and 190 cm<sup>-1</sup> are assigned to the T<sub>2g</sub> mode of the regular octahedron.

In a first attempt to identify the six internal stretching modes of the W-O atoms in the distorted WO<sub>6</sub> octahedra of ZnWO<sub>4</sub>, Liu *et al.* [23] assigned them to the modes at 906, 787 and 407 cm<sup>-1</sup> on the basis of the bond lengths and Raman frequencies in the WO<sub>6</sub> group. Afterwards, Wang *et al.* [24] assigned the internal stretching modes to the phonons observed near 906, 787, 709, 407, 342, and 190 cm<sup>-1</sup> on the basis of the temperature dependence of the Raman frequencies. However, this assignment is in contradiction with the fact that the frequencies of the internal modes are expected to be higher than those of the external modes. These authors argue in favor of their assignment that the oxygen sharing between WO<sub>6</sub> and ZnO<sub>6</sub> octahedra may cause a considerable overlap in the frequency range for the two types of vibrations.

### 3.4. Photoluminescence

**Figure 5** shows the representative PL spectra of the ZnWO<sub>4</sub> crystallites synthesized by the hydrothermal method for 2, 4, 6 and 8 h. With the excited wavelength at 320 nm, the corresponding emission peaks centered at ~500 nm can be observed. Obviously, the ZnWO<sub>4</sub> nanorods, prepared at the same calcining temperature (180°C) with a shorter holding time, exhibit lower emission intensity than that from longer time. It implies PL properties of the ZnWO<sub>4</sub> nano-rods are strongly affected by their long scale. This broad emission band had a shoulder in the blue region, indicating it consisted of more than one emission band. The PL spectra were fit to three peaks using a Gauss function as shown in **Figure 6**.

The PL spectrum for the ZnWO<sub>4</sub> film also consisted of an emission band at 2.50 eV (495 nm) and two emission

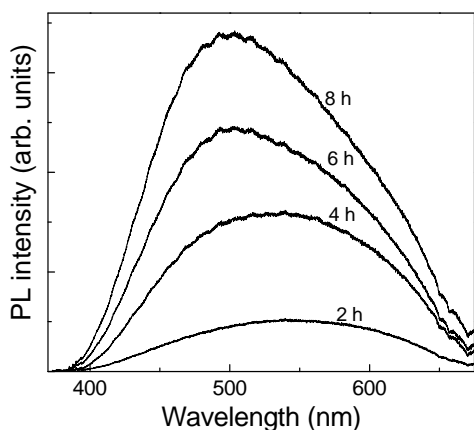


Figure 5. PL spectra ZnWO<sub>4</sub> nanopowders.

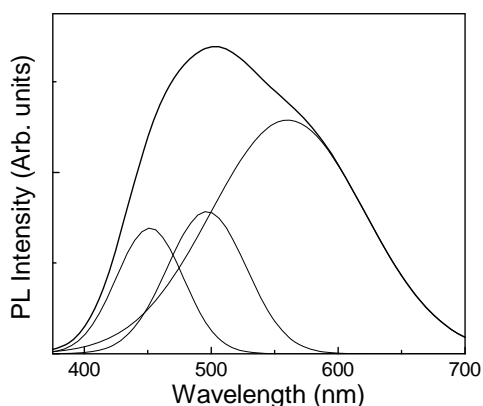


Figure 6. The PL spectra were fit to three peaks using a Gauss function. To clarify, we shows only fitting for PL of the sample with reaction time of 8 h.

bands at 2.80 eV (448 nm) and 2.28 eV (545 nm). To clarify, we show only the fitting figure of the sample with reaction time for 8 h.

It is well established that the  $W_6^{6-}$  complex and a slight deviation from perfect order in the crystal structure are responsible for the emission bands [25]. But there exist different opinions concerning the origin of these bands. Lammers [26] and Grigorjeva [27] believed that the blue and green emissions originated from the intrinsic  $W_6^{6-}$  complex with a double emission from one and the same center ( ${}^3T_{1u} \rightarrow {}^1A_{1g}$ ), whereas the yellow emission is due to recombination of e-h pairs localized at oxygen atom deficient tungstate ions. However, Ovechkin [28] ascribed the blue band to the self-trapped exciton in tungstenite crystals with strong electron-phonon coupling, and the green and yellow bands to the transitions of  $T_{2u} \rightarrow T_{2g}$  and  $T_{1g} \rightarrow T_{2g}$  in the  $W_6^{6-}$  complex. Almost all investigations in luminescent properties of ZnWO<sub>4</sub> have been carried out for large crystals and films. The nanosized ZnWO<sub>4</sub> prepared via a hydrothermal route in the current work showed luminescent properties similar

to those of bulk ZnWO<sub>4</sub>. The luminescence intensities varied from sample synthesized for 2 h to sample synthesized for 8 h. Nanorods with a longer synthesized time exhibited a strong luminescence, and nanorods with a shorter synthesized time gave weak luminescence. These results suggest that morphologies and sizes of nanoparticles may affect their luminescence characteristics. Further studies on PL property of the as-prepared ZnWO<sub>4</sub> crystallites are in progress.

#### 4. Conclusions

In conclusion, ZnWO<sub>4</sub> nano-particles were successfully synthesized at 180°C by a hydrothermal route. The morphology and dimension of the ZnWO<sub>4</sub> crystallites were affected by synthesized time. The optical band gap becomes narrower as increasing the reaction time. The improved PL properties of the ZnWO<sub>4</sub> crystallites can be obtained with the increase of the rod scale. Because the crystallite size of ZnWO<sub>4</sub> for the nano rod is far large, therefore, the absorption edge shift cannot result from quantum size effect but prolonged rod.

#### 5. Acknowledgements

This work has been supported by The Vietnam's National Foundation for Science and Technology Development (NAFOSTED).

#### REFERENCES

- [1] F. A. Kröger, "Some Aspects of the Luminescence of Solids," Elsevier, Amsterdam, 1948.
- [2] L. G. V. Uitert, S. Preziosi, "Zinc Tungstates for Microwave Maser Applications," *Journal Applied Physics*, Vol. 33, No. 9, 1962, pp. 2908-2909. [doi:10.1063/1.1702581](https://doi.org/10.1063/1.1702581)
- [3] P. F. Schofield, K. S. Knight and G. Cressey, "Neutron Powder Diffraction Study of the Scintillator Material ZnWO<sub>4</sub>," *Journal Material Science*, Vol. 31, No. 11, 1996, pp. 2873-2877. [doi:10.1007/BF00355995](https://doi.org/10.1007/BF00355995)
- [4] Caprez, P. Meyer, P. Mikhail and J. Hulliger, "New Host-Lattices for Hyperfine Optical Hole Burning: Materials of Low Nuclear Spin Moment," *Material Research Bull.*, Vol. 32, No. 8, 1997, pp. 1045-1054. [doi:10.1016/S0025-5408\(97\)00070-6](https://doi.org/10.1016/S0025-5408(97)00070-6)
- [5] N. Klassen, S. Shmurak, B. Red'kin, B. Ille, B. Lebeau, P. Lecoq and M. Schneegans, "Correlations between Structural and Scintillation Characteristics of Lead and Cadmium Tungstates," *Nuclear Instrument Methods Physics Research A*, Vol. 486, No. 1-2, 21, June 2002, pp. 431-436.
- [6] M. Itoh, N. Fujita and Y. Inabe, "X-Ray Photoelectron Spectroscopy and Electronic Structures of Scheelite- and Wolframite-Type Tungstate Crystals," *Journal Physics Society Japanese*, Vol. 75, 2006, pp. 084705-084712. [doi:10.1143/JPSJ.75.084705](https://doi.org/10.1143/JPSJ.75.084705)
- [7] J. C. Brice, P. A. C. Whiffin, "Solute Striae in Pulled

- Crystals of Zinc Tungstate,” *British Journal Applied Physics*, Vol. 18, No. 5, 1967, pp. 581-586.  
[doi:10.1088/0508-3443/18/5/304](https://doi.org/10.1088/0508-3443/18/5/304)
- [8] A. R. Phani, M. Passacantando, L. Lozzi and S. Santucci, “Structural Characterization of Bulk ZnWO<sub>4</sub> Prepared by Solid State Method,” *Journal Material Science*, Vol. 35, No. 19, 2000, pp. 4879-4883.  
[doi:10.1023/A:1004809804206](https://doi.org/10.1023/A:1004809804206)
- [9] L. Honeycutt and A. Kuzmin, J. Purans “Communication and Design Course; Local atomic and electronic structure of tungsten ions in AWO<sub>4</sub> Crystals of Scheelite and Wolframite Types,” *Radiat Measurement*, Vol. 33, No. 5, 2001, pp. 583-586.
- [10] A. Henglein, “Estimated Distributions of Electronic Redox Levels in aq/e<sub>aq</sub><sup>-</sup>, H<sub>aq</sub><sup>+</sup>/H<sub>aq</sub> and Some Other Systems,” *General Introductory Chemistry*, Vol. 78, No. 10, 1974, pp. 1078-1084.  
[doi:10.1002/bbpc.19740781016](https://doi.org/10.1002/bbpc.19740781016)
- [11] M. Bonanni, L. Spanhel, M. Lerch, E. Fuglein and G. Muller, “Conversion of Colloidal ZnO-WO<sub>3</sub> Heteroaggregates into Strongly Blue Luminescing ZnWO<sub>4</sub> Xerogels and Films,” *Chemistry Material*, Vol. 10, No. 1, 1998, pp. 304-310. [doi:10.1021/cm9704591](https://doi.org/10.1021/cm9704591)
- [12] F.-S. Wen, X. Zhao, H. Huo, J.-S. Chen, E. Shu-Lin and J.-H. Zhang, “Hydrothermal Synthesis and Photoluminescent Properties of ZnWO<sub>4</sub> and Eu<sup>3+</sup>-Doped ZnWO<sub>4</sub>,” *Materials Letters*, Vol. 55, No. 3, 2002, pp. 152-157.  
[doi:10.1016/S0167-577X\(01\)00638-3](https://doi.org/10.1016/S0167-577X(01)00638-3)
- [13] M. H. Huang, S. Mao, H. Feick, H. Yan, Y. Wu, H. Kind, E. Weber, R. Russo and P. Yang, “Room-Temperature Ultraviolet Nanowire Nanolasers,” *Science*, Vol. 292, 2001, pp. 1897-1899. [doi:10.1126/science.1060367](https://doi.org/10.1126/science.1060367)
- [14] Y. Cui and C. M. Lieber, “Functional Nanoscale Electronic Devices Assembled Using Silicon Nanowire Building Blocks,” *Science*, Vol. 291, 2001, pp. 851-853.  
[doi:10.1126/science.291.5505.851](https://doi.org/10.1126/science.291.5505.851)
- [15] K. Kuribayashi, M. Yoshimura, T. Ohta and T. Sata, “Processes in the Reaction of Yttrium Oxide with Tungsten Trioxide,” *Bull Chemistry Sciences Japanese*, Vol. 50, No. 11, 1977, pp. 2932-2934.  
[doi:10.1246/bcsj.50.2932](https://doi.org/10.1246/bcsj.50.2932)
- [16] R. C. Pullar, S. Farrah and N. M. Alford, “MgWO<sub>4</sub>, ZnWO<sub>4</sub>, NiWO<sub>4</sub> and CoWO<sub>4</sub> Microwave Dielectric Ceramics,” *Journal of the European Ceramic Society*, Vol. 27, No. 2-3, 2007, pp. 1059-1063
- [17] H. Fu, J. Lin, L. Zhang and Y. Zhu, “Photocatalytic Activities of a Novel ZnWO<sub>4</sub> Catalyst Prepared by a Hydrothermal Process,” *Applied Catalysis A: General*, Vol. 306, No. 7, 2006, pp. 58-67.  
[doi:10.1016/j.apcata.2006.03.040](https://doi.org/10.1016/j.apcata.2006.03.040)
- [18] K. N. P. Kumar, K. Keizer and A. J. Burggraaf, “Textural Evolution and Phase Transformation in Titania Membranes: Part 1 Unsupported Membranes,” *Journal Material Chemistry*, Vol. 3, No. 11, 1993, pp. 1141-1149.  
[doi:10.1039/jm9930301141](https://doi.org/10.1039/jm9930301141)
- [19] X. Zhao, W. Yao, Y. Wu, S. Zhang, H. Yang and Y. Zhu, “Fabrication and Photoelectrochemical Properties of Porous ZnWO<sub>4</sub> Film,” *Journal of Solid State Chemistry*, Vol. 179, No. 8, 2006, pp. 2562-2570.
- [20] M. A. Butler, “Photoelectrolysis and Physical Properties of the Semiconducting Electrode WO<sub>2</sub>,” *Applied Physics*, Vol. 48, No. 5, 1977, pp. 1914-1920.
- [21] M. Bonanni, L. Spanhel, M. Lerch, E. Fuglein and G. Muller, “Conversion of Colloidal ZnO-WO<sub>3</sub> Heteroaggregates into Strongly Blue Luminescing ZnWO<sub>4</sub> Xerogels and Films,” *Chemics Material*, Vol. 10, No. 1, 1998, pp. 304-310. [doi:10.1021/cm9704591](https://doi.org/10.1021/cm9704591)
- [22] A. Kalinko and A. Kuzmin, “Raman and Photoluminescence Spectroscopy of Zinc Tungstate Powders,” *Journal of Luminescence*, Vol. 129, No. 10, 2009, pp. 1144-1147.  
[doi:10.1016/j.jlumin.2009.05.010](https://doi.org/10.1016/j.jlumin.2009.05.010)
- [23] Y. Liu, H. Wang, G. Chen, Y. D. Zhou, B. Y. Gu and B. Q. Hu, “Analysis of Raman spectra of ZnWO<sub>4</sub> single crystals,” *Journal Applied Physics*, Vol. 64, No. 9, 1988, pp. 4651-4653. [doi:10.1063/1.341245](https://doi.org/10.1063/1.341245)
- [24] H. Wang, F. D. Medina, Y. D. Zhou and Q. N. Zhang, “Temperature Dependence of the Polarized Raman Spectra of ZnWO<sub>4</sub> Single Crystals,” *Physics Reviews B*, Vol. 45, No. 18, 1992, pp. 10356-10362.  
[doi:10.1103/PhysRevB.45.10356](https://doi.org/10.1103/PhysRevB.45.10356)
- [25] G. Blasse, M. J. J. Lammers and D.S. Robertson, “Structure and Bonding, the Luminescence of Cadmium Tungstate (CdWO<sub>4</sub>),” *Physics Status Solidi A*, Vol. 63, 1981, pp. 569-572.
- [26] L. Grigorjeva, R. Deych, D. Millers and S. Chernov, “Time-Resolved Luminescence and Absorption in CdWO<sub>4</sub>,” *Radiation Measurement*, Vol. 29, No. 3-4, 1998, pp. 267-271.
- [27] A. E. Ovechkin, V. D. Ryzhikov, G. Tamulaitis and A. Žukauskas, “Luminescence of ZnWO<sub>4</sub> and CdWO<sub>4</sub> Crystals,” *Physics Status Solidity A*, Vol. 103, No. 1, 1987, pp. 285-290. [doi:10.1002/pssa.2211030133](https://doi.org/10.1002/pssa.2211030133)